Theoretical and Applied Genetics (2023) 136:68
https://doi.org/10.1007/s00122-023-04271-8

ORIGINAL ARTICLE

A 5.5-kb LTR-retrotransposon insertion inside phytochrome B gene (*CsPHYB*) results in long hypocotyl and early flowering in cucumber (*Cucumis sativus* L.)

Liangliang Hu[1] · Miaomiao Zhang[1] · Jingjing Shang[3] · Zichen Liu[1] · Yiqun Weng[2] · Hongzhong Yue[4] · Yuhong Li[1] · Peng Chen[3]

Received: 13 July 2022 / Accepted: 2 January 2023 / Published online: 23 March 2023

Abstract

Key message **The novel spontaneous *long hypocotyl* and *early flowering* (*lhef*) mutation in cucumber is due to a 5551-bp LTR-retrotransposon insertion in *CsPHYB* gene encoding PHYTOCHROME B, which plays a major role in regulating photomorphogenic hypocotyl growth and flowering.**

Abstract Hypocotyl length and flowering time are important for establishing high-quality seedlings in modern cucumber production, but little is known for the underlying molecular mechanisms of these two traits. In this study, a spontaneous cucumber *long hypocotyl* and *early flowering* mutant was identified and characterized. Based on multiple lines of evidence, we show that cucumber *phytochrome B* (*CsPHYB*) is the candidate gene for this mutation, and a 5551-bp LTR-retrotransposon insertion in the first exon of *CsPHYB* was responsible for the mutant phenotypes. Uniqueness of the mutant allele at *CsPHYB* was verified in 114 natural cucumber lines. Ectopic expression of the *CsPHYB* in Arabidopsis *phyB* mutant rescued the long hypocotyl and early flowering phenotype of *phyB*-9 mutant. The wild-type CsPHYB protein was localized on the membrane and cytoplasm under white light condition, whereas in the nucleus under red light, it is consistent with its roles as a red-light photoreceptor in Arabidopsis. However, the mutant csphyb protein was localized on the membrane and cytoplasm under both white and red-light conditions. Expression dynamics of *CsPHYB* and several cell elongation-related genes were positively correlated with hypocotyl elongation; the transcription levels of key positive and negative regulators for flowering time were also consistent with the anthesis dates in the mutant and wild-type plants. Yeast two hybrid and bimolecular fluorescence complementation assays identified physical interactions between CsPHYB and phytochrome interacting factor 3/4 (CsPIF3/4). These findings will provide new insights into the roles of the *CsPHYB* in cucumber hypocotyl growth and flowering time.

Introduction

Light is not only the major driver of plant photosynthesis, but also arguably one of the most important environmental cues that profoundly regulate plant growth and development (Xu et al. 2019; Yadav et al. 2020). Plants perceive the light signals through a set of sophisticated photoreceptors, which include the red and far red light-absorbing phytochromes (phyA-phyE) (Oh et al. 2020; Kahle et al. 2020), blue/UVA light-absorbing cryptochromes (CRY1 and CRY2) (Miao et al. 2022; Xu et al. 2021; Zhong et al. 2021), phototropins (PHOT1 and PHOT2) (Inoue et al. 2020; Rusaczonek et al. 2021) and UVB light-absorbing UV RESISTANCE LOCUS 8 (UVR8) (Ge et al. 2020; Miao et al. 2021). Among these photoreceptors, the phytochromes (phys) are well characterized that play critical roles in various physiological and developmental processes, including seed germination,

Communicated by Richard G.F. Visser.

✉ Yuhong Li
liyuhong73@nwsuaf.edu.cn

✉ Peng Chen
pengchen@nwsuaf.edu.cn

[1] College of Horticulture, Northwest A&F University, Yangling 712100, Shaanxi, China

[2] Horticulture Department, USDA-ARS Vegetable Crops Research Unit, University of Wisconsin, Madison, WI 53706, USA

[3] College of Life Science, Northwest A&F University, Yangling 712100, Shaanxi, China

[4] Vegetable Research Institute, Gansu Academy of Agricultural Sciences, Lanzhou 730070, Gansu, China

photomorphogenesis and transition to flowering time (Nemhauser and Chory. 2002; Hajdu et al. 2015; Fragoso et al. 2017; Zou et al. 2020; Liu et al 2021a, b).

In *Arabidopsis thaliana*, five family members of phytochromes (phyA-phyE) have been identified that are responsible for mediating plant response to red and/or far-red light signals (Briggs and Olney 2001). Of them, the PHYB is the dominant red-light photoreceptor and a positive regulator of photomorphogenesis (Wei et al. 2021). PHYB has two distinct photoconvertible forms: the inactive red-light absorbing form (Pr) and the active far-red light absorbing form (Pfr) (Quail 2002). The hypocotyl elongation is an earliest event of photomorphogenesis affected by the light signal after the seed germination in plants (Nakano et al. 2019). As a positive regulator of photomorphogenesis, the active form PHYB is directly interacting with a subset of basic helix-loop-helix (bHLH) transcription factors named PHYTOCHROME-INTERACTING FACTORS (PIFs) leading to their rapid phosphorylation, and subsequent degradation via the 26S proteasome pathway, thus inhibiting hypocotyl elongation (Shen et al. 2008; Leivar and Quail 2011). In addition, PHYB can interact with COP1, a RING-finger E3 ubiquitin ligase in a red-light dependent manner to enhance accumulation of bZIP transcription factor HY5 that promotes hypocotyl elongation inhibition (Deng et al. 1992; Jang et al. 2010; Lu et al. 2015; Sheerin et al. 2015). Besides PIFs and COP1, a series of transcriptional regulators were recently identified including the BBX4, SWR1 complex subunits SWC6 and ARP6, MYB30, ARF6/8, AGB1 as the PHYB-interacting protein and downstream components of red light signaling in regulation of the hypocotyl elongation (Xu et al. 2019; Heng et al. 2019; Mao et al. 2020; Yan et al. 2020; Wei et al. 2021).

For all seed crops, the transition from vegetative growth to flowering is a key developmental progress that determines the production of dry matter (Jung and Müller. 2009). In this progress, *PHYB* plays a major role in regulation of flowering in a photoperiod-dependent manner in *Arabidopsis* (Kumar et al. 2018). In photoperiod control of flowering pathway, the positive floral integrator CONSTANS (CO), a CCT domain transcription factor can be promoting flowering by activation of FLOWERING LOCUS T (FT), but degraded by its upstream PHYB to delay flowering under summer long-days in Arabidopsis (Valverde et al. 2004; Song et al. 2015; Kumar et al. 2018). Accordingly, flowering is accelerated in *phyB* mutants (Hajdu et al. 2015). In Arabidopsis *phyB* mutants, the PIF4 basic helix-loop-helix transcription factor was released from and independent of the PHYB and then facilitates the accumulation of FT and promotes flowering (Galvão et al. 2019). In addition, PHYB can also interact directly or indirectly with other proteins including HIGH EXPRESSION OF OSMOTICALLY RESPONSIVE GENES1 (HOS1), PHYTOCHROME AND FLOWERING TIME1 (PFT1) and VASCULAR PLANT ONE–ZINC FINGER1/2 (VOZ1/2) to promote or repress the FT and CO expression level ultimately mediated flowering (Wollenberg et al. 2008; Iñigo et al. 2011; Yasui et al. 2012; Lazaro et al. 2015). These studies suggested that the *PHYB* involved in the regulation of flowering by integrating upstream of some key regulators in the flowering pathway. However, the *PHYB*-mediated flowering was mainly studied in the model plant *Arabidopsis*. In one report in rice, *OsPHYB* functions upstream of *OsCOL4*, a member of the *CONSTANS-like* (*COL*) family to regulate the flowering time was also reported (Lee et al. 2010). Little is known about the *PHYB*-mediated hypocotyl elongation and flowering in other plants. Cloning and characterization of *PHYB* gene from non-model plant species may be useful to improve a better understanding of *PHYB* functions.

Cucumber (*Cucumis sativus* L., $2n = 14$) is an important vegetable crop and cultivated all over the world (Li et al. 2013; Hu et al. 2021). For successful production of cucumber, the use of high-quality seedlings is crucial. The hypocotyl length is closely related to the robust seedlings, which are critical for safe handling, transportation and survival rate after seedling transplanting, and eventually for cucumber yield (Ming et al. 2011). Furthermore, cucumber hypocotyl can be a model organ for exploring the light-mediated cell elongation and photomorphogenesis (Bo et al. 2016; Zhong et al. 2021). For most crops, flowering is also an important agronomic trait directly related to yield and quality (Lu et al. 2014). Commercial cucumbers are generally neutral in photoperiod. Therefore, early flowering is an eminent trait that contributes to the earliness and economic yield in cucumber (Robbins and Staub 2009). Meanwhile, the germplasm with early flowering provides a useful tool to explore the mechanism of the transition from the vegetative phase to the reproductive phase controlled by light signals and genetic pathways. Little is known about the mechanisms by which the *PHYB* controls hypocotyl elongation and flowering time in cucumber. So far, two long hypocotyl genes *elh1* and *lh* were cloned in cucumber (Hu et al. 2021; Liu et al. 2021a, b), but the underlying mechanism of the *elh1* and *lh*-regulated hypocotyl elongation still need further investigation. For flowering time, although a number of QTLs have been identified (Pan et al. 2017; Sheng et al. 2019; Wang et al. 2019), only one candidate gene was identified, which was proposed to be a homolog of Arabidopsis *FT* (Lu et al. 2014). However, the extent and role of *FT* for flowering time in modern cucumber elite cultivars have not been addressed in detail.

Here, we reported identification and characterization of a novel spontaneous mutant with long hypocotyl and early flowering (named as *lhef*). Mapping-based cloning reveled that a 5.5-kb LTR retrotransposon insertion in *CsPHYB* that was responsible for the mutation phenotype, which was a

homolog of Arabidopsis *PHYB* gene participating in the light-induced photomorphogenesis and regulation of flowering time.

Materials and methods

Plant materials and mapping populations

AM274, a.k.a "Salt & Pepper' (Cavatorta et al. 2012) is an inbred line of cultivated cucumber with normal hypocotyl and flowering time (WT or wild type; AM274W hereinafter). A spontaneous mutant with a long hypocotyl and early flowering was identified from AM274W. Since this was the first report on the mutant phenotype in cucumber, the mutant and the underlying gene was referred as AM274M and *lhef* (*long hypocotyl and early flowering*), respectively, hereinafter.

For study of the inheritance of the long hypocotyl and early flowering (*lhef*) locus, F_2 populations were developed from cross of AM274M with three cucumber inbred lines 9930 (North China type), CCMC (a Chinese landrace), and Gy14 (a US pickling type). Initial mapping of the *lhef* locus was performed with 96 AM274M × 9930 F_2 plants. For fine mapping of the *lhef* gene, recombinants were identified from F_2 plants of AM274M × 9930 using flanking markers. All the F_2 plants used for initial mapping and recombinants were self-pollination to produce F_3 offspring. And 40 plants of each F_3 family were examined for segregation of hypocotyl and flowering time to determine F_2 genotype at the *lhef* locus. Segregation of target traits was tested against expected ration with chi-square (χ^2) test. All plants were grown in plastic greenhouses under natural sunlight at the Northwest A&F University (Yangling, China). The length of hypocotyl of all the plants was observed visually and scored at the cotyledon stage.

Flowering time was assessed with the day to anthesis of the first flower (female or male) on each plant after transplanting. The data were collected in both the spring and autumn growing seasons of 2021.

Effects of light quality and temperature on hypocotyl elongation

To explore the effects of light quality and temperature on hypocotyl elongation, the seedlings of AM274M and AM274W were cultured in the growth chambers with different light sources as described in our previous study (Hu et al. 2021). Dark treatment was also employed as a parallel with these experiments. Hypocotyl length was measured at the 15d after germination when the cotyledons were fully expanded. The dynamic change of hypocotyl length and its hypocotyl elongation rate were also investigated every 2 d for 15 days under white and red light, respectively. The effects of temperature on hypocotyl elongation were evaluated at the 18 ℃, 25 ℃ and 32 ℃, respectively. Hypocotyl length was recorded 15d after germination for each treatment.

Microscopic examination of hypocotyl cells

The hypocotyls of AM274W and AM274M were sampled 15d after germination. The center section of the hypocotyl was cut into small pieces and fixed for 24 h at 4 ℃ in FAA solution (acetic acid, formaldehyde, and 70% ethanol by 1:1:18). The fixed samples were stained overnight at 42 ℃ with 1% safranin in 75% ethanol and subsequently dehydrated using series of ethanol concentrations. The samples were then treated with xylene, embedded in paraffin, sectioned with a microtome. The samples were washed with absolute ethanol for 3 min and then stained with 0.1% toluidine blue for 20 min. Paraffin sections were visualized using the BX63 microscope (Olympus, Tokyo, Japan). The hypocotyl cell length and cell numbers were measured or counted using the software ImageJ (https://imagej.nih.gov/ij/).

Fine genetic mapping of *lhef* gene

For quick search, the molecular markers linked with the *lhef* locus, bulked segregation analysis (BSA) was employed in AM274M × 9930 F_2 population for the initial mapping of the *lhef* locus. Two DNA pools were constructed, LH-pool consisting of 10 long hypocotyl and early flowering plants and NH-pool with 10 normal hypocotyl and flowering plants. SSR markers evenly distributed in the seven cucumber chromosomes were chose to screen for polymorphism between the parental lines AM274M and 9930 (Ren et al. 2009). Polymorphic markers were further verified between the two pools and then successively applied to 96 F_2 individuals for linkage analysis.

For fine mapping of the *lhef* locus, the SNP and Indel markers were explored in the target region using high-throughput resequencing reads. Sequence alignment was performed with DNAMAN V10.0 (http://www.lynnon.com/). The SNPs were converted to CAPS and dCAPS markers using dCAPS Finder 2.0 (http://helix.wustl.edu/dcaps/dcaps.html). Additional SSR markers were developed from Sanger sequencing of target DNA region in AM274M and 9930. Primers were designed with Primer Premier 5.0 (http://www.premierbiosoft.com/primerdesign/). Primers were used for various purposes in this study provided in Supplemental Table S1.

DNA extraction, PCR amplification molecular markers and gel electrophoresis were executed as described by Li et al. (2013). Linkage analysis of *lhef* locus with molecular

markers was performed using JoinMap 4.0 at an LOD threshold of 5.0.

Gene prediction and candidate gene identification

The *lhef* locus was finally delimited into a 19.5 kb genomic DNA region in the 9930 (V3.0). This region was manually annotated with the online program FGENESH (http://sunl.softberry.com/). Gene function prediction was performed with BLASTP (https://blast.ncbi.nlm.nih.gov/Blast.cgi). All genes in the target region were Sanger sequenced from AM274M and AM274W to confirm causal polymorphisms.

We found that the mutant phenotype was due to insertion of a 5.5 kb of LTR-RT. To check if this insertion also presented in other cucumber lines, three primers (Table S1) were designed including two (gPHYB-2L and gPHYB-2R) flanking the insertion point and one (gPHYB-IN) within the LTR-RT. These three primers were used to genotype 114 cucumber accessions (Bo et al. 2016) with duplex PCR. The PCR products were resolved with 0.8% agarose gel electrophoresis. Cucumber lines with (mutant) and without (WT) the RT insertion would generate a 439-bp and 217-bp fragment, respectively.

Phylogenetic analysis of *CsPHYB* homologs in plants

We analyzed the phylogenetic relationships of PHYB homologs in 15 plant species (see Supplemental Table S4 for sequences and accession #). Multiple protein sequence alignment was performed with Clustal W, and the phylogenetic tree was constructed with neighbor-joining method (Saitou and Nei. 1987) based on distance calculation with 1000 bootstrap replications in MEGA 7.0 (https://www.megasoftware.net/). Domain structure of CsPHYB protein was predicted using the online tool Batch CD-Search (https://www.ncbi.nlm.nih.gov/Structure/cdd/wrpsb.cgi).

Spatiotemporal expression analysis of *CsPhyb* and other cell elongation and flowering time related genes

Total RNA of hypocotyl samples was extracted from AM274M and AM274W at 3, 5, 7, 9, 11, 13 and 15 days after germination (dag), and cDNA was synthesized using the 5 × All-In-One RT MasterMix (ABM, Canada). Quantitative real-time PCR (qPCR) was performed to examine the time-course expression pattern of the *lhef* gene and other genes (*CsaV3_3G015200* and *CsaV3_3G015210*) in the candidate gene region (19.3 kb). We also examined the expression of *lhef* candidate gene in various cucumber organs including the shoot apical meristem, hypocotyl, root, stem, cotyledon, true leaf, flower and fruit. The cDNA of hypocotyl was also used for *lhef* candidate gene cloning.

To explore the molecular mechanism by which *lhef* regulates hypocotyl elongation and flowering time, we examined the expression of selected genes involved in the cell expansion including *CsEXT3* (*EXTENSIN3*), *CsEXPA8* (*EXPANSIN-A8*), *CsDWF4* (*DWARF4*), *CsXTR6* (*XYLOGLUCAN ENDOTRANSGLYCOSYLASE6*), *CsXTH22* (*XYLOGLUCAN ENDOTRANSGLUCOSYLASE/HYDROLASE PROTEIN22*), *CsPIF3/4* (*PHYTOCHROME-INTERACTING FACTOR 3/4*), *CsCOP1* (*CONSTITUTIVELY PHOTOMORPHOGENIC 1*) and *CsHY5* (*ELONGATED HYPOCOTYL 5*) (Bo et al. 2016; Hu et al. 2021). We also examined gene expression of selected genes known to regulate flowering time in plants including *CsFT* (*FLOWERING LOCUS T*), *CsSOC1* (*SUPPRESSOR OF OVEREXPRESSION OF CONSTANS 1*), *CsCO* (*CONSTANS*), *CsTFL1b* (*TERMINAL FLOWER 1b*), *CsELF3* (*EARLY FLOWERING 3*) and *CsLFY* (*LEAFY*) (Cai et al. 2020). Previous studies in Arabidopsis showed the endogenous gibberellin also was involved in the flowering (Blázquez et al. 1999). Therefore, the expression level of two key genes *CsKAO* (*ent-kaurenoic acid oxidase 1*) and *CsGA20ox-2* (*gibberellin 20 oxidase 2-like*) for bioactive GA biosynthesis, and *CsGA2ox-1* (*gibberellin 2-beta-dioxygenase 1)* encoding GA-inactivating enzyme were also examined in cucumber mutant *lhef*. The *UBI-ep* gene (*ubiquitin extension protein*) was used as the internal reference for qPCR (Wan et al. 2010). Relative expression level of the target gene was calculated using the $2^{-\Delta\Delta Ct}$ method (Livak and Schmittgen. 2001). There were three biological and four technical replicates for each sample.

Subcellular localization of *CsPHYB* and *csphyb* protein

The CDS (coding sequence) of WT and mutant alleles of *CsPHYB* without the stop codons were cloned with the two pairs of gene-specific primers 35S-CsPHYB-L/35S-CsPHYB-R and 35S-csphyb-L/35S-csphyb-R (Table S5), respectively, and inserted into the downstream region of CaMV 35S promoter in vector pCAMBIA3301-EGFP. The constitutive expression *35S:CsPHYB-EGFP* and *35S:csphyb-EGFP* vectors were used for transient expression in tobacco (*N. benthamiana*) leaves following Li (2011). The empty vector pCAMBIA3301-EGFP was used as the negative control. After two days of incubation, fluorescence was observed under white or red light. The EGFP fluorescence was observed using an Olympus BX63 fluorescence microscope.

Ectopic expression of CsPhyB in Arabidopsis

The *35S:CsPHYB-EGFP* plasmid construct described above was used to transferred into *Agrobacterium tumefaciens*

GV3101 and then transformed to WT (Col) and *phyb* mutant Arabidopsis plants by floral dip (Clough and Bent. 1998). The T1 transgenic plants were screened by spraying Basta solution (0.0015%) (Bayer, Germany) every three days (Hu et al. 2021), which were further confirmed by PCR. Hypocotyl length and flowering time of transgenic plants were measured and recorded.

Yeast two-hybrid (Y2H) and bimolecular fluorescence complementation (BiFC) assays

The transcription factors *PIF3/4* play an important role in regulation of photomorphogenesis-related hypocotyl elongation and flowering (Oda et al. 2004; Galvão et al. 2019; Heng et al. 2019; Xu et al. 2019). In order to explore the underlying regulatory pathway of *CsPHYB*-mediated hypocotyl growth and flowering in cucumber, the protein–protein interactions were investigated using Y2H and BIFC for CsPHYB and CsPIF3/4. Full-length CDS of WT *CsPHYB*, N-terminal and C-terminal of the *CsPHYB* and mutant *csphyb* gene were PCR amplified and fused into the pGBKT7 bait vector. The CDS of *CsPIF3/4* was amplified and inserted into pGADT7 vector (prey vector). For BiFC assays, full length CDS of *CsPHYB* was cloned and fused into pCAMBIA1302-nYFP; full-length CDS of *CsPIF3* and *CsPIF4* without the stop codon were cloned and fused into pCAMBIA1302-cYFP vector, respectively. The two constitutive plasmids for test of a specific interaction were transformed into *Agrobacterium tumefaciens* strain GV3101 and then co-transformed into 3-5-week-old tobacco leaves. After 48 h, the GFP signal was observed and imaged under an Olympus BX63 fluorescence microscope.

Results

Phenotypic characterization of *lhef* mutant

In growth chamber, the *lhef* mutant exhibited much longer hypocotyl and earlier flowering time than the WT (Figs. 1a, b, 2a–c, S1). Under field conditions, the mutant had pale-green leaves, elongated petioles and internodes; it was also taller than WT (Figs. 1c, d, 2d, S2, S3a-d). In 2021 spring and autumn field observations, the mutant flowered 5–7 days earlier than the WT in both seasons (Figs. 2a–c, S3a-b). The *lhef* shared a similar morphological phenotype for long hypocotyl and early flowering to some previously characterized *phyB* mutants in Arabidopsis (Koornneef et al 1980; Reed et al. 1993).

We compared cell size and number of hypocotyls from 15d-old *lhef* and WT seedlings grown under white and red (R) lights. Under the microscope, we found that, under both light conditions, the mutant and WT had similar cell numbers (Fig. 1j), but the mutant had much longer longitudinal cells than the WT (Fig. 1e-i). The result indicated that the longer hypocotyl of *lhef* mutant was due primarily to the longitudinal elongation of cells.

Hypocotyl elongation of *lhef* under different light quality and temperature

We compared the dynamics of hypocotyl growth between *lhef* mutant and WT under white and R lights (Figs. S4a-b, S5a-b). The hypocotyl length and elongation rate of *lhef* mutant were all significantly higher than that of WT at any time point (Figs. S4b-c, S5b-c); the elongation rate reached the peak at the 7d after germination in both lines (Figs. S4c, S5c). We further investigated the hypocotyl growth under monochromic red (R), far-red (FR), blue lights, as well as in the dark, and found that the *lhef* and WT seedlings exhibited similar elongation of the hypocotyl in FR, blue light and dark (Fig. 3) suggesting white and R lights inhibit hypocotyl elongation in WT but not in the mutant. Thus, this mutant may be blind to red light response or signal transduction.

We investigated the effect of temperature on hypocotyl elongation of *lhef* mutant and WT at 18 ℃, 25 ℃ and 32 ℃ (Fig. S6a–c). Hypocotyl elongation was inhibited in both lines at higher (32 ℃) and lower (18 ℃) temperatures as compared with that at optimal growth temperature (25 ℃) (Fig. S6). However, the hypocotyl length of *lhef* mutant was higher than WT at all three temperatures (Fig. S6d). These data suggested that hypocotyl elongation was mainly affected not only by the endogenous genes, but also the light and temperature.

Genetic characterization and linkage mapping of *lhef* mutant

We investigated the inheritance of hypocotyl length and flowering in segregating populations derived from AM274M. F_1 plants of AM274M × 9930 and AM274M × Gy14 displayed short hypocotyl and normal flowering time (Table 1). Among 8246 AM274M × 9930 F_2 plants, 6150 had normal hypocotyl and flowering time, 2096 had long hypocotyl and early flowering fitting 3 WT to 1 mutant segregating ratio ($P = 0.380$ in χ^2 test) (Table 1). There was no recombination between the two traits (that is, long hypocotyl with normal flowering or short hypocotyl with early flowering) suggesting both traits are due to pleiotropic effects of the same mutant locus. In the AM274M × Gy14 F_2 population, among 6352 plants scored, 4711 had normal hypocotyl and flowering time, and 1614 had long hypocotyl and early flowering time ($P = 0.342$ in χ^2 test against 3:1 segregation ratio) (Table 1). These data supported that the long hypocotyl and early flowering in AM274M was controlled by a single recessive gene *lhef*.

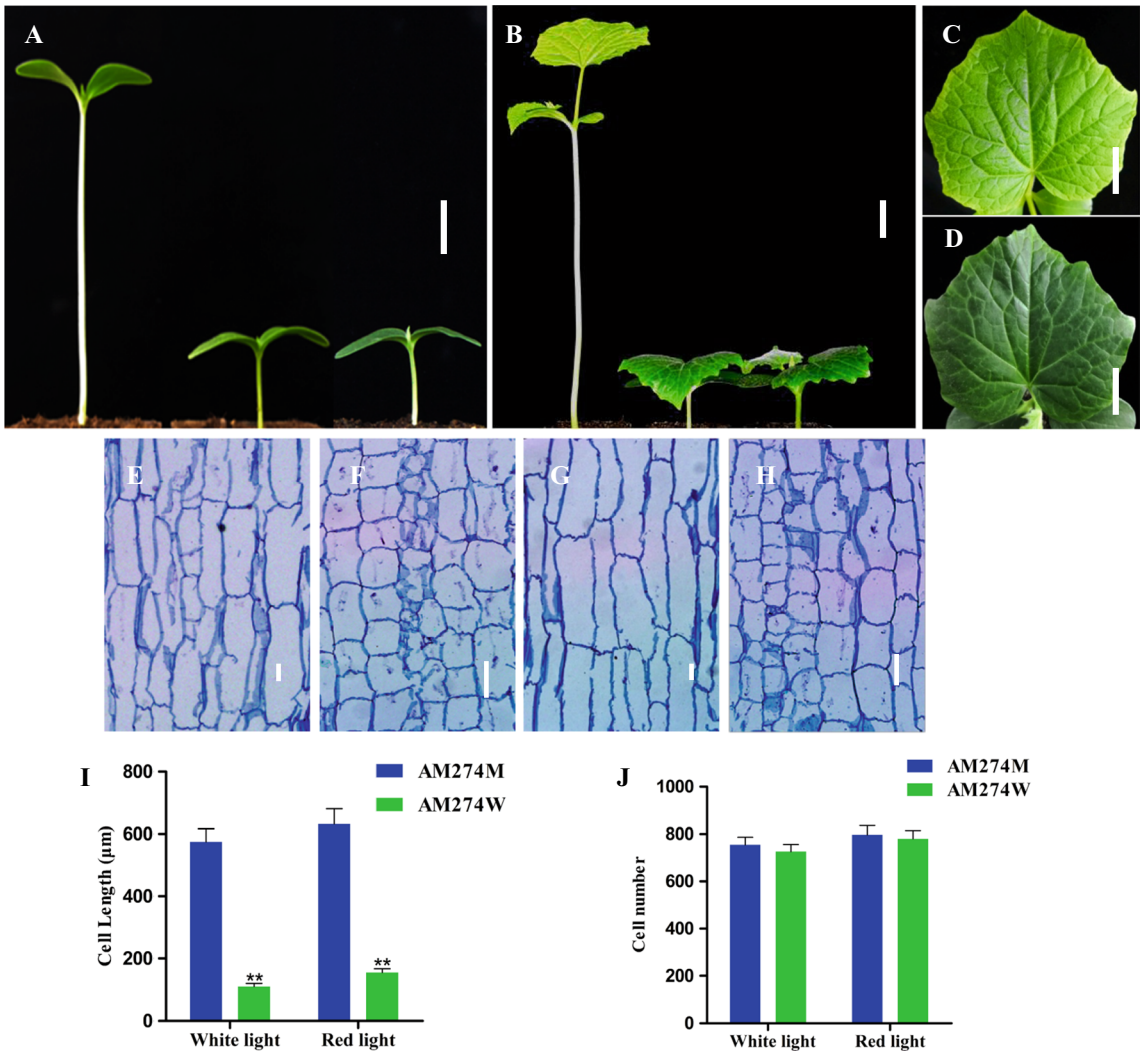

Fig. 1 Hypocotyl phenotype of mutant AM274M and wild-type (WT) AM274W. **a** and **b** are hypocotyls of the mutant (left), WT (middle) and their F_1 (right) at the cotyledon stage and first true leaf stage, respectively; **c** and **d** are leaf color of mutant (**c**) and WT (**d**). Scale bar = 2 cm. Micrographs of hypocotyl cells of 15d-old seedling of mutant (**e**) and WT (**f**) under white light condition, and mutant (**g**) and WT (**h**) under red light condition. The mutant has significantly longer cell length (**i**), while the similar cell numbers (**j**) as compared with the WT either white light or red-light condition. Scale bar = 100 μm. Data are means ± SD. **Means $P < 0.01$ from Student's *t* test

For linkage mapping of *lhef*, 1653 SSR markers were screened among 9930 and AM274M, from which 140 were found polymorphic between AM274M and 9930. Six of the 140 markers were also polymorphic between the LH-pool and NH-pool, all of which were located on chromosome (Chr) 3 (Table S1). Linkage analysis with 96 F_2 plants of AM274 × 9930 confirmed linkage of the six markers with the *lhef* locus (Fig. 4a). One additional SSR maker, SSR03918 was identified between the SSR02771 and SSR04570. A framework genetic map was developed with the 7 markers and 96 F_2 plants; the *lhef* locus was located between SSR03918 and SSR04570, which were 2.6 and 3.2 cM away from *lhef*, respectively (Fig. 4a).

For fine mapping, we expanded the population size to 8246 F_2 plants of AM274M × 9930. Meanwhile, additional eight polymorphic SSR markers were mined between the initial flanking markers SSR03918 and SSR04570. Subsequently, we screened all 8246 F_2 plants with flanking markers and identified 65 recombinants between marker UW024-5 and UW024-4 (Fig. 4b). The two markers flanked the *lhef* locus in a ~ 84.1 kb genomic DNA region (Table S1).

To further narrow down the candidate gene region, Indels and SNPs identified from Sanger sequencing of selected DNA fragments from the ~ 84.1 kb region, which were converted to Indel and CAPS/dCAPS markers, respectively. Four markers (dCAPS024-1, dCAPS024-2,

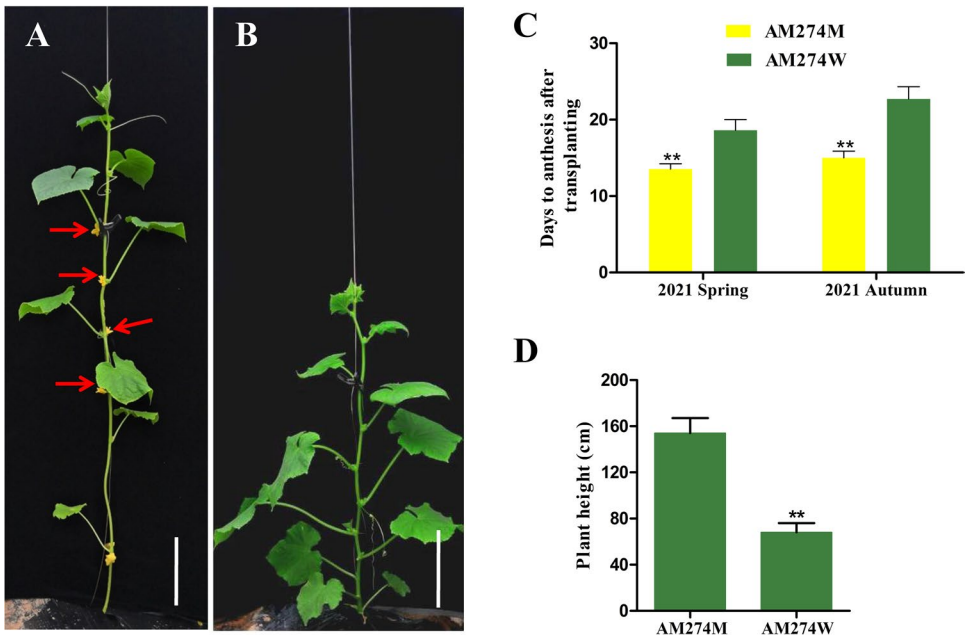

Fig. 2 Flowering time performance of mutant AM274M (**a**) and wild-type AM274W (**b**); Date of first flower (either male or female flower) after transplanting of AM274M ($n=200$) and wild-type AM274W ($n=200$) in spring and autumn of 2021, respectively (**c**). The plant height of mutant AM274M was significantly higher than WT under the field condition (**d**). Scale bar = 20 cm. Each data point is mean ± SD. $^{**}P<0.01$ in Student's *t* test

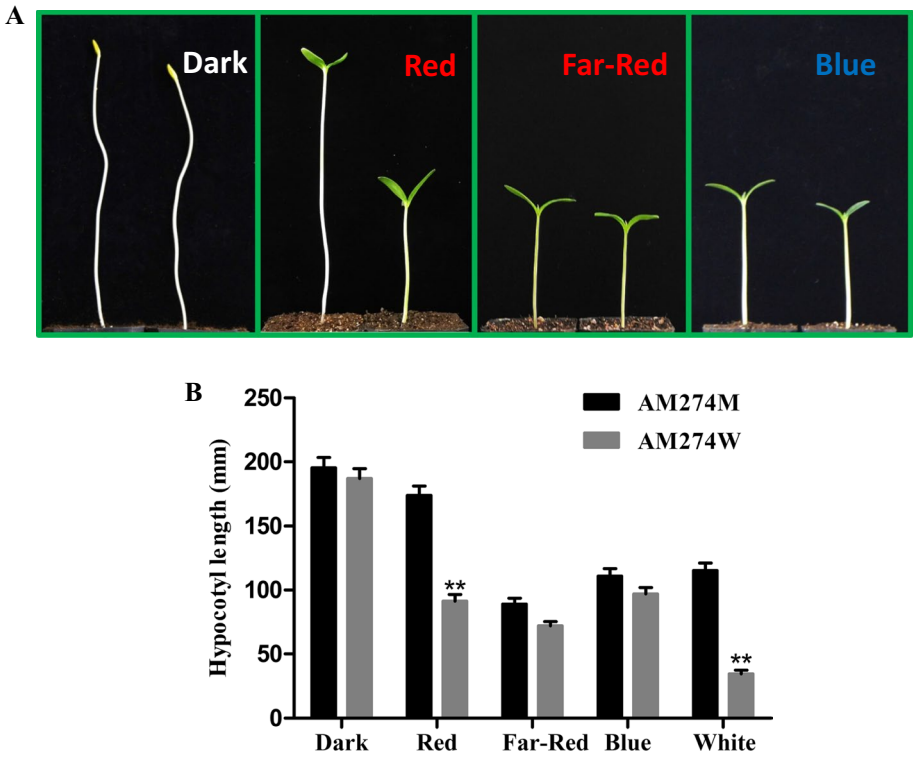

Fig. 3 Hypocotyl growth of mutant AM274M and WT AM274W under different light conditions. **A** shows the difference of hypocotyl elongation in mutant AM274M (left) and WT AM274W (right) under dark, red, far-red and blue lights, respectively. Hypocotyl length data of 15-d old seedling of mutant AM274M and WT AM274W grown as described in (**a**) were collected (**b**). Data are means ± SD. **Means $P<0.01$ significant level in Student's *t* test from comparisons between mutant AM274M and WT AM274W at different light condition

Indel024-1 and dCAPS024-3) were added in this region. The resulting genetic map for the *lhef* locus with fourteen markers is shown in Fig. 4b. Finally, the *lhef* locus was delimited to a ~ 19.3 kb region flanked by Indel024-1 and dCAPS024-3 (Fig. 4b; Table S1).

Cloning and prediction in the *lhef* locus region

The FGENESH program predicted three genes in the *lhef* region including *CsaV3_3G015200, CsaV3_3G015210*, and *CsaV3_3G015190* (Fig. 4c). Information about the

Table 1 Segregation analysis of long hypocotyl and early flowering in F_1 and F_2 populations from various crosses

Populations	Total	Wild type	Mutant	Expected ration	*P* in χ^2 tests
AM274M × CCMC F_1	82	82	0	1:0	–
AM274M × 9930 F_1	76	76	0	1:0	–
AM274M × Gy14 F_1	58	58	0	1:0	–
AM274M × CCMC F_2	1278	946	332	3:1	0.419
AM274M × 9930 F_2	8246	6150	2096	3:1	0.380
AM274M × Gy14 F_2	6325	4711	1614	3:1	0.342

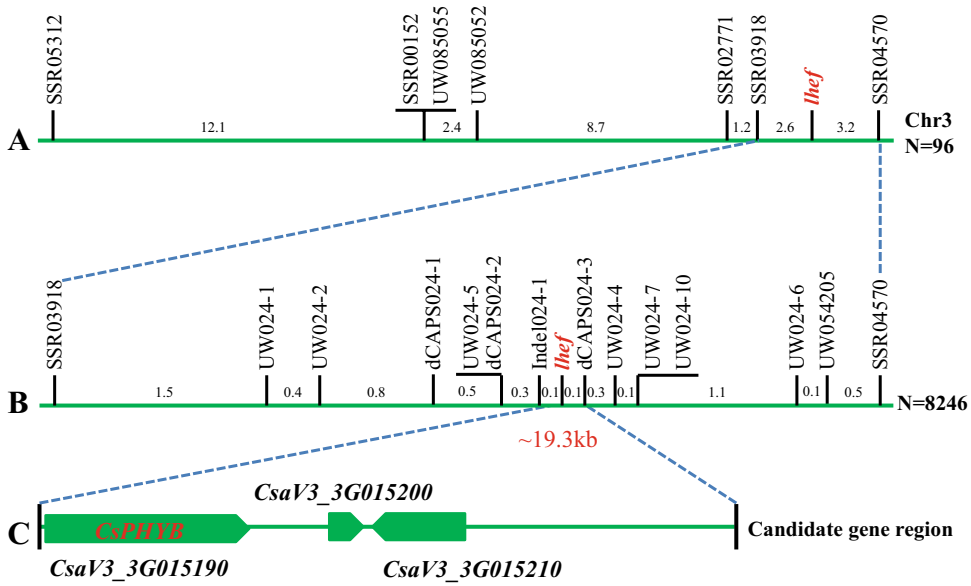

Fig. 4 Mapping-based cloning of the *lhef* locus in cucumber. **a** *lhef* was mapped initially with 96 $F_{2:3}$ families to the cucumber chromosome 3 between markers SSR03918 and SSR04570. **b** Fine mapping with 8246 F_2 plants narrowed *lhef* to a ~ 19.3 kb region flanked by two markers Indel024-1 and dCAPS024-3. The numbers in **a** and **b** represent the genetic distances (cM) between two adjacent markers. **c** In the ~ 19.3 kb region, three genes were predicted and the *CsPHYB* (first) as the candidate gene

three genes is presented in Supplemental Table S2. The CDS and ~ 2000 bp sequence upstream of transcription start of the three genes were cloned from both AM274W and AM274M. No sequence variation in *CsaV3_3G015200* and *CsaV3_3G015210* was found. But a large long-terminal-repeat retrotransposon (LTR-RT) insertion was identified inside this gene (*CsaV3_3G015190*) that encodes Phytochrome B (*CsPHYB*). We also examined the expression of the three genes in the hypocotyls of AM274W and AM274M. Only *CsaV3_3G015190* showed differential expression between the two lines (Fig. 6a–d; see details below). The long hypocotyl and early flowering phenotypes of the *lhef* were also similar to *phyB* mutants reported in Arabidopsis (Koornneef et al 1980; Reed et al. 1993). These data suggested that *CsaV3_3G015190/CsPHYB* is the most possible candidate gene for *lhef*.

The loss of function mutation in *CsPHYB* is due to insertion of a 5.5-kb LTR retrotransposon

Four primer pairs were designed to clone the *CsPHYB* genomic DNA sequences from AM274M and AM274W (Fig. S7). Interestingly, amplification for the second fragment of *CsPHYB* failed in AM274M. Through many attempts and trials and errors, we finally identified and cloned a 5551-bp LTR-RT insertion in the first exon of the *CsPHYB* resulting in a 10,511-bp fragment in the mutant (Fig. 5b; Supplemental file 1). In addition to the 5.5 kb insertion, no sequence difference inside *CsPHYB* was found between AM274W and AM274M. The complete sequences of the *CsPHYB* (4960 bp) in AM274W and *Csphyb* (10,511-bp) in AM274M are provided in the Supplemental file 1.

The 5551-bp insertion had a typical retrotransposon structure (Fig. 5c; Supplemental file 1): it was flanked by a 5-bp Target Site Duplication (TSD) sequence (5′-GCAAT-3′) and contained a pair of 256-bp long terminal repeats (LTRs) at 5′ and 3′ ends. This LTR-RT had five exons and four introns predicted to encode five conserved protein domains typical of LTR-RTs that included RNase_HI_RT_Ty1, RVT_2, Transpos_IS481, GAG_pre-integrs and Retrotran_gag (Fig. 5c) (Boeke and Corces 1989). In the plants genomes, this LTR-RT belongs to the class I/Copia type TE according to the classification of transposable elements (TE) (Wicker et al. 2007).

We also cloned full length cDNA sequences from AM274M and AM274W using gene specific

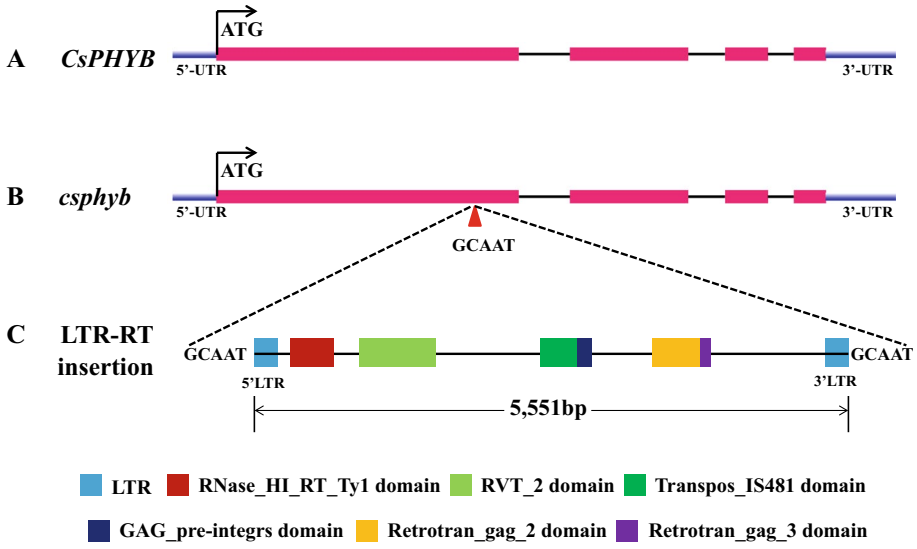

Fig. 5 Predicted gene structure of the wild-type AM274W (**a**) and mutant AM274M (**b**) alleles of *CsPHYB* candidate gene (Phytochrome B) and annotated 5551-bp LTR retrotransposon (**c**). Boxes and lines indicate exons and introns, respectively. There are four exons in the predicted gene, and the mutant allele is due to insertion of 5551-bp LTR-RT at the first exon (**b**). The LTR-RT is predicted to encode all protein domains required for active transposition (**c**)

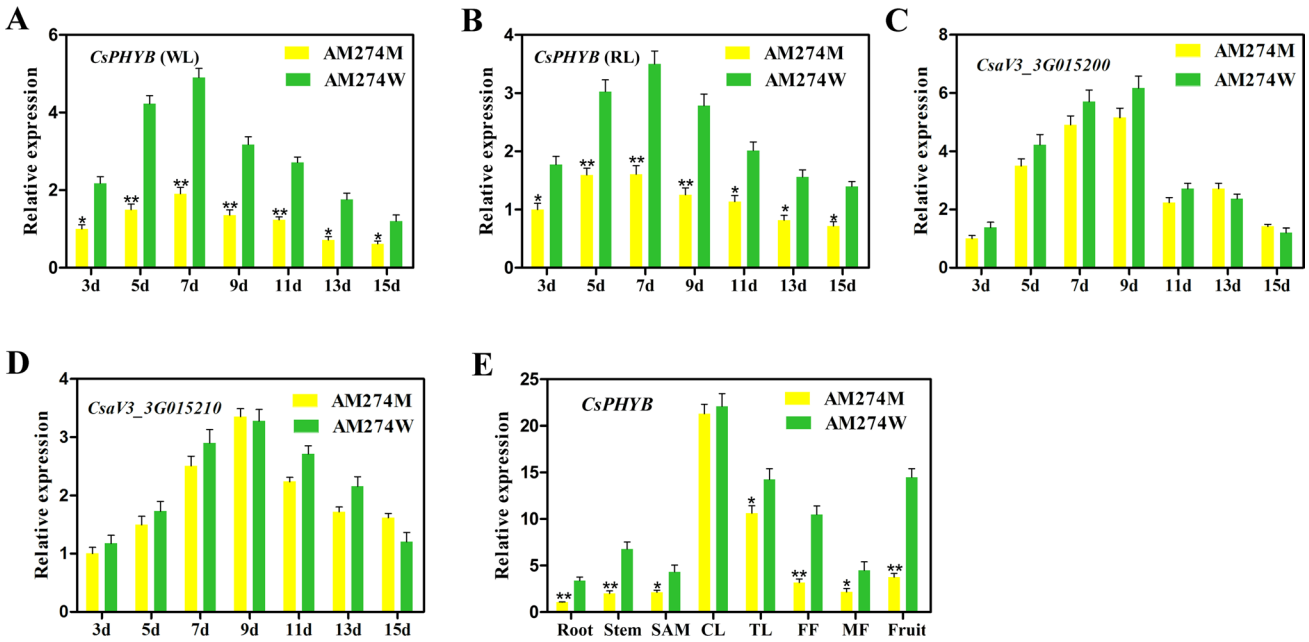

Fig. 6 RT-PCR assessment of *CsPHYB* in the WT and mutant. **a**, **b** Time-course expression of *CsPHYB* candidate gene within 15d after germination under white and red-light condition, respectively. **c**, **d** Expression dynamics of other two genes in the ~ 19.3 kb region. Expression levels of these three genes in third day of mutant AM274M were regarded as their respective standard of "relative" expression. **e** Transcriptional level of *CsPHYB* in eight different tissues (*SAM* shoot apical meristem, *CL* cotyledon, *TL* true leaf, *FF*/*MF* female/male flower), the expression of *CsPHYB* in root of mutant was used as the standard of "relative" expression. Values shown are mean ± SD of three biological and three technical replicates. *$P < 0.05$ and **$P < 0.01$ by Student's *t*-test

primers CsPHYB-L and CsPHYB-R. Alignment of cDNA sequences between the mutant *Csphyb* (3660 bp) and WT *CsPHYB* (3399 bp) revealed extra 261-bp sequence in the first exon in the mutant, which introduced a stop codon and thus a premature protein (Supplemental file 2 and 3). These data suggested that the mutation phenotype in AM274M is due to the 5551-bp LTR-RT insertion in *CsPHYB*.

Allelic diversity at *lhef* locus in natural populations

For further verify the identity of the 5551-bp LTR-RT insertion with the long hypocotyl and early flowering mutation in AM274M, the uniqueness of this LTR-RT insertion inside CsPhyB in both segregating and natural cucumber populations. Based on the 5551-bp LTR-RT insertion, three primers were designed for duplex PCR. We first genotyped the

AM274M × 9930 F_2 plants and AM274M × Gy14 F_2 plants, which confirmed that the 5551-bp LTR-RT insertion and the co-segregation of phenotypes for long hypocotyl and early flowering in both populations (Figs. 4b, S8). Duplex PCR was also employed using genomic DNAs of 114 cucumber accessions including AM274, of which 113 had WT hypocotyl. All accessions had the 217-bp fragment (WT) except AM274M that had a 439-bp (Fig. S9). This work provided additional evidence that the 5551-bp LTR-RT insertion in *CsPHYB* was indeed the casual mutation for the long hypocotyl phenotype in AM274M.

Phylogenetic analysis of *CsPHYB* in other species with similar functions

To better understand the structural and functional relationships among CsPHYB in cucumber and PHYB proteins from other plant species, a phylogenic tree was constructed using the amino acid sequences of PHYB from 15 species (Table S4; Fig. S10). In the phylogenic tree, the position of different plant species represents the evolutionary relationship among them. Amino acid sequence alignment showed that most PHYB proteins had identical conserved domains (Supplemental file 4) suggesting conserved functions of this gene in different species. The positions where the 5551-bp LTR-RT insertion mutation occurred in PHY domain of CsPHYB were highly conserved in different species. This could explain the similar phenotypes of PHYB mutants in different plant species (e.g., long hypocotyl and early flowering) (Koornneef et al 1980; Reed et al. 1993; Takano et al. 2005; Kippes et al. 2020).

Expression pattern of *lhef* candidate gene, cell elongation and flowering time related genes

We examined the expression level of *CsPHYB* from the mutant *lhef* and WT hypocotyl samples at different time points after germination under white and R light (Fig. 6a, b). The expression of *CsPHYB* was positively correlated with hypocotyl elongation rate under both light conditions (Figs. 6a, b, S4c, S5c). In the mutant, the transcriptional level was significantly reduced compared with the WT at any point time (Fig. 6a, b). We also examined the expression of *CsPHYB* in different organs with qPCR, which was the highest in the cotyledon and true leaves, followed by fruit, female and male flowers, stem, shoot apical meristem and root (Fig. 6e). In all organs except the cotyledons, its expression was significantly higher in the WT than in the mutant (Fig. 6e). These results suggest that the reduced expression of *CsPHYB* gene may be responsible for the long hypocotyl, early flowering, pale-green leaves, elongated stem and petioles in the mutant.

In order to explore the underlying molecular mechanism by *CsPHYB*-mediated hypocotyl elongation and early flowering, we examined the expression level of five cell-elongation related genes (*CsEXT3*, *CsEXPA8*, *CsDWF4*, *CsXTR6* and *CsXTH22*) and four key players regulating photomorphogenesis (*CsPIF3/4*, *CsHY5* and *CsCOP1*). All five cell-elongation related genes had the highest expression at the seventh day, which was consistent with the hypocotyl elongation rate (Figs. 7a–e, S4c). Meanwhile, in the mutant *CsPIF3/4* and *CsCOP1* had higher expression and *CsHY5* had lower expression than in the WT (Fig. 7f–i). These results suggest that expression of all these genes except *CsHY5* was positively collated with hypocotyl cell elongation, while *CsHY5* may be involved in hypocotyl cell elongation inhibition in cucumber.

The expression of several genes known to regulate flowering in plants was also examined with qPCR. Four genes promoting flowering including *CsFT*, *CsSOC1*, *CsCO* and *CsLFY* were all significantly up-regulated in the mutant than in WT; two negative regulators of flowering time, *CsTFL1b* and *CsELF3* were down-regulated in the mutant (Fig. 7j). Additionally, the expression of *CsKAO* and *CsGA20ox-2* responsible for bioactive GA biosynthesis was significantly higher but the GA-inactivating gene *CsGA2ox-1* was significantly lower in the mutant than that in WT (Fig. 7j). These data indicated that *CsPHYB* also may be a crucial regulator of flowering time in cucumber.

Subcellular localization of *CsPHYB* protein

Subcellular localization of CsPHYB and csphyb protein was performed in tobacco leaves cells. The fluorescence of the negative control (35S:EGFP) was present at the cytomembrane and nucleus. The fusion protein 35S:CsPHYB-EGFP was localized on the membrane and cytoplasm under white light condition (Fig. 8a), whereas in the nucleus under red light (Fig. 8b), it is consistent with PhyB's roles as a red light photoreceptor in Arabidopsis. However, the fusion mutant protein 35S:csphyb-EGFP was localized on the membrane and cytoplasm under both white and red light conditions (Fig. 8a, b). We speculate that upon absorption of red light, the CsPHYB not the csphyb can convert the inactive Pr form into the Pfr active form and translocated into the nucleus, where it plays a crucial role in regulation of hypocotyl elongation and flowering through interacting with a series of transcriptional regulator.

Ectopic expression of *CsPHYB* decreased the hypocotyl length and rescued the early flowering phenotype in *Arabidopsis mutant*

To explore the function of CsPHYB in hypocotyl elongation and flowering time, we introduced *CsPHYB* driven by the

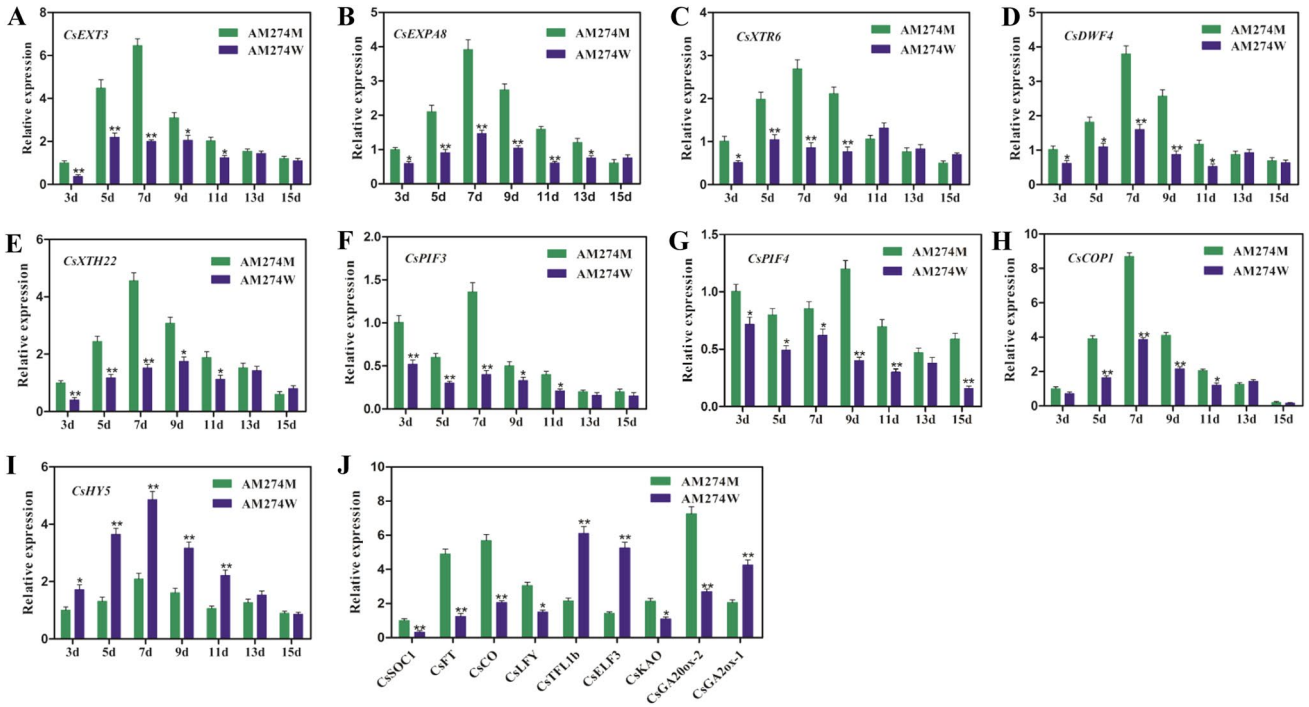

Fig. 7 Expression profiles of five cell-elongation related genes (**a–e**) and four crucial regulators of photomorphogenesis (**f–i**). For all eight genes (**a–h**), the expression level was significantly up-regulated in mutant AM274M; the positive regulator of hypocotyl elongation inhibition HY5 (**i**) was down-regulated expression in mutant AM274M, which was consistent with increased hypocotyl elongation under white light condition. Expression levels of six key genes in flowering pathway of mutant AM274M and WT were examined, respectively (**j**). Two key genes *CsKAO* and *CsGA20ox-2* for bioactive GA biosynthesis were significantly up-regulated expression, but the GA-inactivating gene *CsGA2ox-1* was significantly down-regulated in mutant *lhef* than that in WT (**j**). Data are means ± SD of three biological and three technical replicates. Asterisks indicate statistically significant differences at $*p < 0.05$ and $**p < 0.01$ by Student's *t*-test

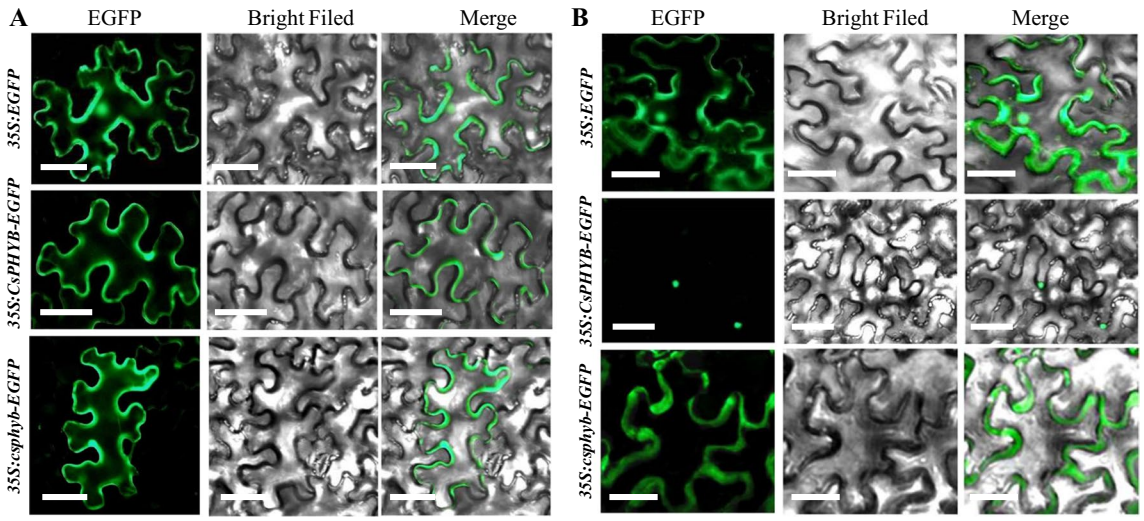

Fig. 8 Subcellular localization of CsPHYB and csphyb in epidermal cells of *Nicotiana benthamiana* leaves. **a**, **b** CsPHYB is localized in membrane and cytoplasm under white light and in the nucleus under red light; csphyb is localized in membrane and cytoplasm both under white and red light conditions. Scale bar = 50 um

CaMV35S promoter into Arabidopsis *phyB*-9 mutant. Ten independent T1 transgenic lines carrying the *35S:CsPHYB* construct were obtained, of which three representative complementation lines were further analyzed for hypocotyl length and flowering time (Fig. 9c). The hypocotyl length of transgenic lines was significantly decreased compared with that the Arabidopsis *phyB-9* mutant (Fig. 9a, d). The Arabidopsis *phyB-9* mutant showed early flowering, and overexpression of the *CsPHYB* can rescue the early flowering phenotype of the *phyB-9* mutant, and delay its flowering (Fig. 9b, e–f). These results further supported the roles of cucumber *CsPHYB* in regulation of hypocotyl elongation and flowering time.

CsPHYB physically interacts with *CsPIF3/4* to regulate hypocotyl growth and flowering

As the red-light photoreceptor, PHYB protein plays a pivotal role in regulation of plant photomorphogenesis-related hypocotyl elongation and flowering (Mockler et al. 1999; Wei et al. 2021). PIF3/4 acts antagonistically with the PHYB (Su et al. 2015; Xu et al. 2019). We examined interactions between CsPHYB and CsPIF3/4 with yeast two-hybrid (Y2H) assays. We found that the CsPHYB has auto-activation ability, whereas csphyb lost this ability (Fig. 10a) suggesting that the 5551-bp LTR-RT insertion in *CsPHYB* causes the loss of transcriptional activity in the mutant. We further fount that the C-terminal but not the N-terminal of CsPHYB could interact with CsPIF3/4 in vitro (Fig. 10a). However, no interaction was found between mutated csphyb protein and CsPIF3/4 (Fig. 10a). The interaction between CsPIF3/4 and CsPHYB was further validated with BiFC (bimolecular fluorescence complementation) assay. GFP (Green fluorescent protein) fluorescence signals could be observed only when CsPHYB and CsPIF3/4 were co-expressed in the nucleus of tobacco leaf epidermal cells (Fig. 10b, c). These results suggest that the CsPHYB, not the csphyb, may interact with CsPIF3/4 to promote or inhibit the expression of downstream cell elongation and flowering-related genes,

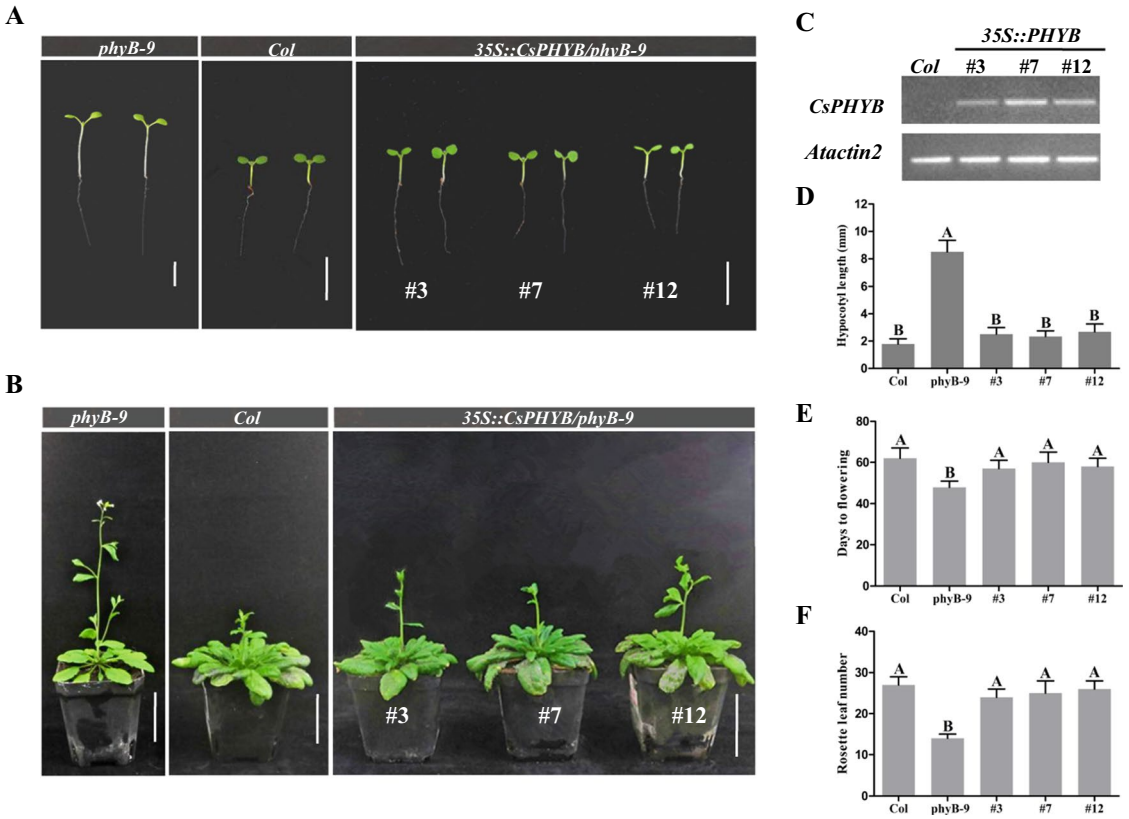

Fig. 9 Phenotypic characterization of 35S:*CsPHYB* transgenic plants in *Arabidopsis*. **a** Hypocotyl elongation of *CsPHYB* overexpression plants in *phyb-9* mutant. **b** Flowering time of *CsPHYB* overexpression plants in *phyb-9* mutant. **c** Transcript level in three independent *CsPHYB* transgenic plants based on semi-RT-PCR. **d–f** The statistical analysis of hypocotyl length (**d**), days to flowering (**e**) and rosette leaf number (**f**) in *Arabidopsis CsPHYB* transgenic lines. The capital letters A and B indicate statistically significant differences in *t* tests at $P < 0.01$

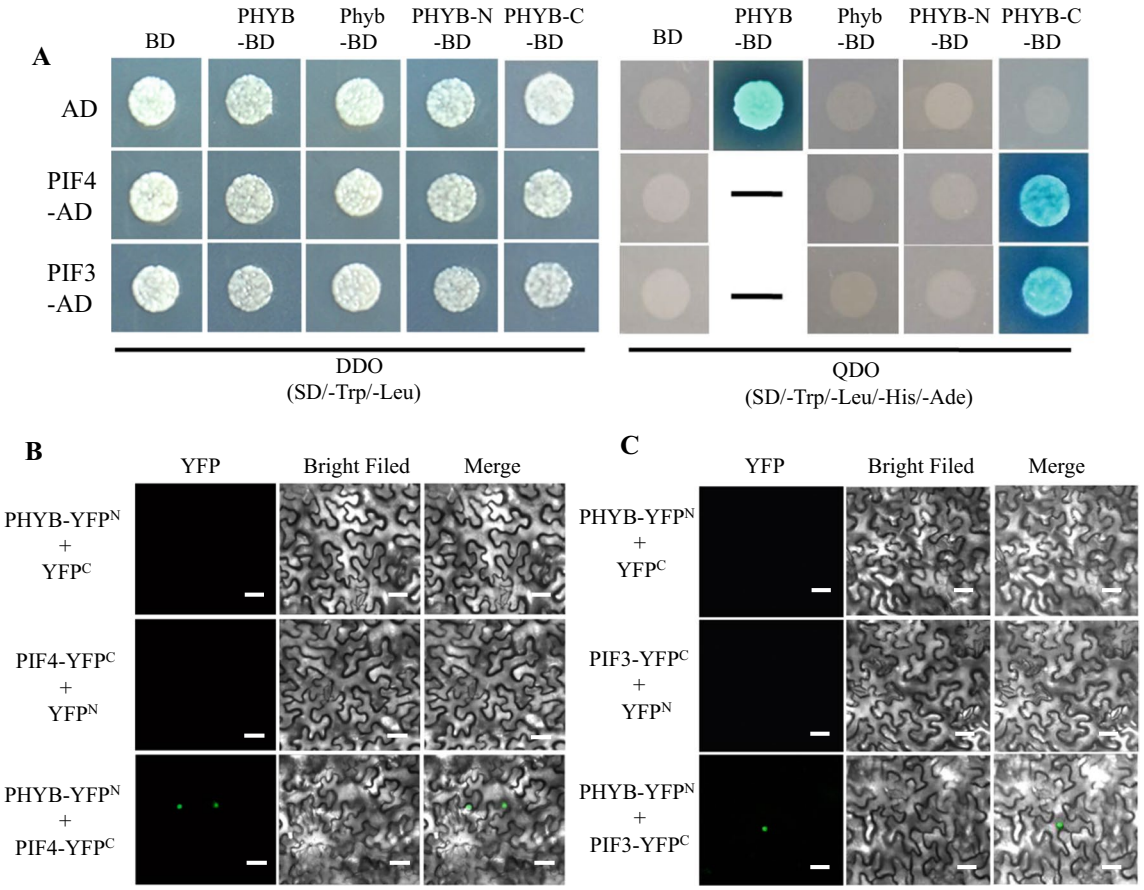

Fig. 10 Yeast two-hybrid (Y2H) and bimolecular fluorescence complementation (BiFC) assays. **a** C-terminal of CsPHYB can interaction with the CsPIF3/4 in vitro. **b**, **c** BiFC assay showing the interaction of CsPHYB with CsPIF3/4 in the nuclear. CsPHYB and CsPIF3/4 were fused to the N- and C-terminal fragments of YFP (YFPN and YFPC, respectively). Unfused YFPN and YFPC fragments served as negative controls. Scale bars = 100 μm

thereby regulating hypocotyl elongation and flowering (Figs. 7a–e, j, 10).

Discussion

In the present study, we cloned the *lhef* locus from the spontaneous mutant AM274M and showed that mutation in *CsPHYB* was responsible for the long hypocotyl and early flowering in the mutant. Our conclusion was based on several lines of evidence. First, similar to the Arabidopsis *phyB* mutant, the cucumber *lhef* mutant is blind to the white and R light response and thus exhibited long hypocotyl and early flowering (Figs. 1, 2, 3). Second, we delimited the *lhef* locus to a 19.3 kb region by the map-based cloning strategy (Fig. 4c). Among three predicted genes in the 19.3 kb region, only *CsPHYB* exhibited a polymorphism between the mutant and WT which was a 5551-bp LTR-RT insertion in the first exon of *CsPHYB* resulting in a stop codon and thus a premature protein (Figs. 4, 5, S7; Supplemental file 1–3). Third, the time-course expression pattern of the *CsPHYB* in the hypocotyl was well consistent with the hypocotyl elongation rate under white and R light (Figs. 6a, b; S4c, S5c). However, expression level of other two genes in 19.3 kb region had no difference between mutant *lhef* and WT at any time point (Fig. 6c, d). Fourth, three primers for duplex PCR confirmed its complete co-segregation with the long hypocotyl and early flowering mutant phenotype in two large F_2 segregating populations (Figs. 4c, S8). Further, Allelic analysis among 114 cucumber lines indicated the uniqueness of the 5551-bp LTR-RT insertion in *lhef* (Fig. S9). Lastly, ectopic expression of *CsPHYB* in Arabidopsis was able to rescue the long hypocotyl and early flowering phenotype of the *phyB-9* mutant (Fig. 9). Taken together, these data provided convincing evidence in support of *CsPHYB* as the candidate gene of *lhef*.

The plant phyB protein consists of two modules: the N-terminal photosensory and the C-terminal dimerization moieties, both of which are essential for light signaling (Nagatani 2010; Pearce et al. 2016). The N-terminal

photosensory core module, which binds an open tetrapyrrole chromophore, is comprised of three domains: PHY (Phytochrome-specific) domain, GAF (cGMP phosphodiesterase, Adenylyl cyclase, FhlA) domain and the PAS (PER, ARNT and SIM) (PAS)—like domain (Nagatani 2010; Pearce et al. 2016). The C-terminal module includes two successive PAS domains and a HKRD domain (histidine-kinase-related domain), which is responsible for PHYB dimerization and is indispensable to downstream regulatory functions (Wagner et al. 1996). In this study, the 5551-bp LTR-RT insertions in the first exon of *CsPHYB* not only leads to the N-terminal structural variation, but also complete loss of the C-terminal functional domain (Supplemental files 3–4). Previous studies found that mutations in either N-terminal or C-terminal of PHYB protein would result in loss-of-function to red light perception and photoperiodic response (Koornneef et al 1980; Reed et al. 1993; Suzuki et al. 2011; Takano et al. 2005; Kippes et al. 2020). For example, all reported *phyB* mutants including Arabidopsis *phyB-1* to *phyB-10* (Koornneef et al 1980; Reed et al. 1993; Franklin and Quail. 2010; Yoshida et al. 2018), tomato $tri^{1/2/3/4}$ (Tuinen et al. 1995), *Brassica rapa ein* (Devlin et al. 1992), rice *elc-1*/2/3/4/5 (also named *phyB-1* to *phyB-5*) (Takano et al. 2005), sorghum ma_3 and ma_3^R (Childs et al. 1997; Lee et al. 1998a), and wheat *phyB-null* mutant (Kippes et al. 2020) exhibited common mutation phenotypes with long hypocotyl and early flowering as in the cucumber *lhef* mutant identified herein (Figs. 1, 2). These reports further supported that the cucumber *CsPHYB* has conserved functions in regulating hypocotyl elongation and flowering time as in other plant species in a red light and photoperiod-dependent manner, respectively.

However, unlike other reported *phyB* mutants that were caused by deletion, T-DNA insertion or non-synonymous SNPs in *PHYB* gene (Koornneef et al 1980; Devlin et al. 1992; Reed et al. 1993; Tuinen et al. 1995; Childs et al. 1997; Takano et al. 2005; Kippes et al. 2020), we here reported a novel allelic mutation in cucumber *CsPHYB* gene that was caused by a LTR-RT insertion. LTR-RTs are a class of transposable elements (TE) that are abundant in plants, which can fall inside or close to genes, and thus influence their expression and evolution (Galindo-González et al. 2017). As expected, we found the significantly down-regulated expression of *CsPHYB* in the mutant compared to the WT at different time-point of hypocotyl elongation, as well as in different organs (Fig. 6a, b, e). More significantly, the LTR-RT insertion event also provides a new insight in the evolution of *CsPHYB*-mediated hypocotyl elongation and flowering time in cucumber.

Phenotypically, Arabidopsis *phyB* mutants have reduced leaf areas compared with the WT (Koornneef et al 1980; Reed et al. 1993), which was not observed in the cucumber mutant *lhef* and the WT (Fig. 1c, d) suggesting possibly different regulation mechanism of *PHYB* in leaf development between Arabidopsis and cucumber. However, similar to the Arabidopsis and rice mutants, the cucumber *lhef* mutant also displays light green leaves with a reduced chlorophyll content under white and red light (Fig. S2b-c), indicating that the similar functions for *PHYB*-mediated red signal positively regulates chlorophyll biosynthesis among different plant species.

It was worth noting that the *lhef* mutant not only had longer hypocotyl, but also longer internode length than the WT (Fig. S2a) thus resulting in taller plant (Fig. 2d). This suggests that the *PHYB* also plays an important role in stem elongation and plant height of cucumber. We also found that the cucumber *lhef* mutant had fewer lateral branches compared with the WT at the field condition (Figs. S3a-b, S3e). Limited studies have been done on the genetic basis of lateral branch development in cucumber. The mutant we described herein may provide a useful tool to explore genetics of lateral branch development in cucumber, which is a very important horticulture trait for cucumber breeding.

In an early study (Hu et al. 2021), we reported the *elongated hypocotyl1* (*elh1*) mutant caused by a mutation in *CsHY2* encoding the phytochromobilin (PΦB) synthase for phytochromes biosynthesis. The *elh1* mutant exhibits higher female/male flower ratios than its wild-type CCMC, which was not found in the *lhef* mutant reported herein. The suggests that deficiency of all phytochromes as found in the *elh1* mutant, rather than the loss of function in *CsPHYB* as seen in the *lhef* mutant contributes to increased femaleness in cucumber.

In this study, we identified positive protein–protein interactions between CsPHYB and the transcriptional regulator PIF3/4 (Fig. 10). In Arabidopsis, PIF3/4 regulates the expression of downstream target genes through binding to G-box (CACGTG) /E-box (CANNTG) motif of target genes promoters (Huq and Quail. 2002; Sun et al. 2020). Indeed, the expression levels of several genes containing G-box/E-box in promoters related to cell elongation and flowering time were all changed in the mutant AM274M (Fig. 7). Among them, *CsKAO* and *GA20ox-2* for active gibberellin (GA) biosynthesis were significantly up-regulated, and the GA metabolism gene *CsGA2ox-2* was significantly down-regulated expression in the mutant compared with the WT (Fig. 7j). As expected, the GA concentration of phytochrome B-deficient mutant AM274M was significantly higher than WT in the hypocotyl (data not shown) supporting the critical role of GAs in cucumber hypocotyl elongation (Hu et al. 2021). It has also been reported that the PHYB and GA have opposite effects on flowering in Arabidopsis and sorghum: PHYB delays flowering while GAs promote flowering (Lee et al. 1998a, b; Blázquez and Weigel 1999; Endo et al. 2005; Fukazawa et al. 2021). In the present study, in addition to promoting hypocotyl elongation, GA also stimulates flowering in cucumber because the mutant AM274M and WT

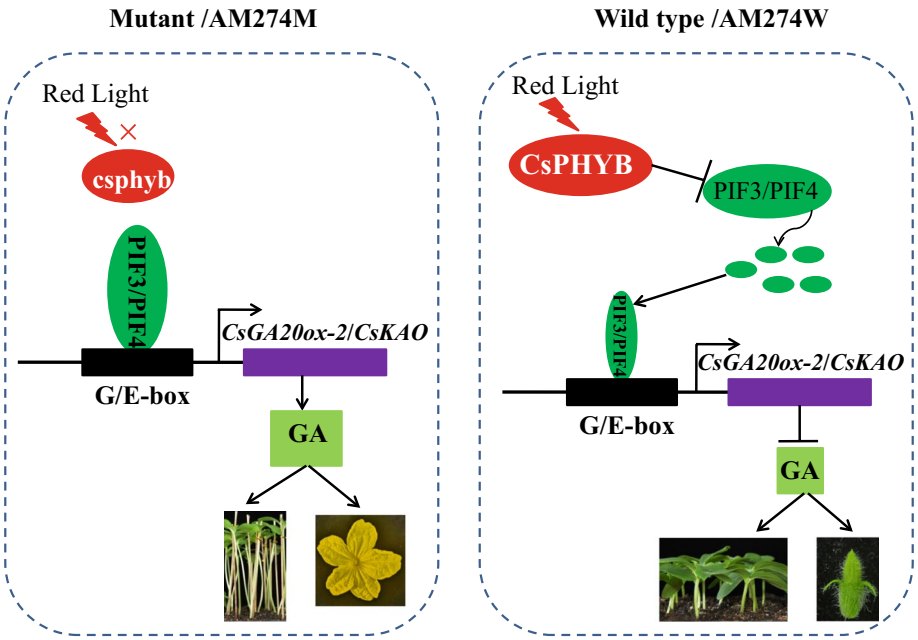

Fig. 11 A working model for illustrating the underlying predicted mechanisms of LHEF-regulated hypocotyl elongation and flowering through modulating of the GA biosynthesis in the mutant AM274M and wild-type AM274W. **a** In the long hypocotyl and early flowering mutant AM274M, the csphyb is unable to sense the red light signaling and cannot interact with PIF3/4 in the nucleus, which strongly binds to the promoter region of *CsKAO* and *CsGA20ox-2* to promote GA biosynthesis, resulting in the hypocotyl elongation and early flowering in AM274M plants. **b**. In the short hypocotyl and later flowering wild-type AM274W, the CsPHYB can sense the red light signaling and transfer into the nucleus from the membrane and cytoplasm to interact with the PIF3/4 resulting in the down-regulated expression of PIF3/4. The lower abundance of PIF3/4 weakly binding to the promoter of *CsKAO* and *CsGA20ox-2* results in lower GA concentrations and thus represses the hypocotyl elongation and early flowering

displayed both longer internodes and early flowering under treatment with 100 µmol GA, and exhibited shorter internodes and delaying flowering treated with 100 µmol PAC when compared with their mock treatment (Fig. S11). Thus, we proposed a working model for *lhef/CsPHYB* in regulating hypocotyl elongation and flowering (Fig. 11). CsPHYB perceives the red light signaling and then interacts with CsPIF3/4, which inhibits the binding of CsPIF3/4 to the promoters of *CsKAO* and *CsGA20ox-2* to repress the GA biosynthesis, and ultimately promotes the hypocotyl elongation inhibition and delay flowering in WT (Fig. 11).

To summarize, we identified a LTR-RT insertion in the *lhef/CsPHYB* gene that is responsible for long hypocotyl and early flowering in AM274M mutant. The *lhef* gene may be involved in photomorphogenesis-related hypocotyl growth and flowering by response to the light signaling. These results would provide useful information for understanding the mechanisms of *lhef* mediating stem elongation and flowering time in cucumber. However, the relationships between *lhef* and other hypocotyl growth and flowering-related genes deserves further investigation.

Supplementary Information The online version contains supplementary material available at https://doi.org/10.1007/s00122-023-04271-8.

Acknowledgements Work in PC's and HY's lab was supported by the National Natural Science Foundation of China under Project #31860557. YL's lab was supported by the National Natural Science Foundation of China under Project #31772300. YW's lab was supported by the Agriculture and Food Research Initiative competitive Grant No. 2017-67013-26195 of the USDA National Institute of Food and Agriculture.

Author contribution statement LH performed the research and prepared a draft of the manuscript. MZ, JS, ZL and YW participated in the research. HY participated in data analysis and provided technical help. YL and PC designed the experiments, supervised this study and revised the manuscript with inputs from YW. All authors have read and approved the manuscript.

Declarations

Conflict of interest The authors declare that there is no conflict of interest.

Data availability All data generated or analyzed that support the findings of this study are included in the main text article and its supplementary files.

References

Blázquez MA, Weigel D (1999) Independent regulation of flowering by phytochrome B and gibberellins in Arabidopsis. Plant Physiol 120:1025–1032

Bo KL, Wang H, Pan YP, Behera TK, Pandey S, Wen CL, Wang YH, Simon PW, Li YH, Chen JF, Weng YQ (2016) *SHORT HYPOCOTYL1* encodes a SMARCA3-like chromatin remodeling factor regulating elongation. Plant Physiol 172:1273–1292

Boeke JD, Corces VG (1989) Transcription and reverse transcription of retrotransposons. Annu Rev Microbiol 43:403–434

Briggs WR, Olney MA (2001) Photoreceptors in plant photomorphogenesis to date: five phytochromes, two cryptochromes, one phototropin, and one superchrome. Plant Physiol 125:85–88

Cai YL, Bartholomew ES, Dong MM, Zhai XL, Yin S, Zhang YQ, Feng ZX, Wu LC, Liu W, Shan N, Zhang X, Ren HZ, Liu XW (2020) The HD-ZIP IV transcription factor GL2-Like regulates male flowering time and fertility in cucumber. J Exp Bot 71:5425–5437

Cavatorta J, Moriarty G, Glos M, Henning M, Kreitinger M, Mazourek M, Munger H, Jahn J (2012) Salt and pepper': a disease-resistant cucumber Inbred. HortSci 47:427–428

Childs KL, Miller FR, Cordonnier-Pratt MM, Pratt LH, Morgan PW, Mullet JE (1997) The sorghum photoperiod sensitivity gene, Ma3, encodes a phytochrome B. Plant Physiol 113:611–619

Clough SJ, Bent AF (1998) Floral dip: a simplified method for *Agrobacterium*-mediated transformation of *Arabidopsis thaliana*. Plant J 16:735–743

Deng XW, Matsui M, Wei N, Wagner D, Chu AM, Feldmann KA, Quail PH (1992) *COP1*, an arabidopsis regulatory gene, encodes a protein with both a zinc-binding motif and a G_β homologous domain. Cell 71:791–801

Devlin PF, Rood SB, Somers DE, Quail PH, Whitelam GC (1992) Photophysiology of the *elongated internode* (*ein*) mutant of brassica *rapa*: *ein* mutant lacks a detectable phytochrome B-like polypeptide. Plant Physiol 100:1442–1447

Endo M, Nakamura S, Araki T, Mochizuki N, Nagatani A (2005) Phytochrome B in the mesophyll delays flowering by suppressing *FLOWERING LOCUS T* expression in Arabidopsis vascular bundles. Plant Cell 17:1941–1952

Fragoso V, Oh Y, Kim SG, Gase K, Baldwin IT (2017) Functional specialization of *Nicotiana attenuata* phytochromes in leaf development and flowering time. J Integr Plant Biol 59:205–224

Franklin KA, Quail PH (2010) Phytochrome functions in Arabidopsis development. J Exp Bot 61:11–24

Fukazawa J, Ohashi Y, Takahashi R, Nakai K, Takahashi Y (2021) DELLA degradation by gibberellin promotes flowering via GAF1-TPR-dependent repression of floral repressors in Arabidopsis. Plant Cell 33:2258–2272

Galindo-González L, Mhiri C, Deyholos MK, Grandbastien MA (2017) LTR-retrotransposons in plants: engines of evolution. Gene 626:14–25

Galvão VC, Fiorucci AS, Trevisan M, Franco-Zorilla JM, Goyal A, Schmid-Siegert E, Solano R, Fankhauser C (2019) PIF transcription factors link a neighbor threat cue to accelerated reproduction in *Arabidopsis*. Nat Commun 10:4005

Ge XM, Hu X, Zhang J, Huang QM, Gao Y, Li ZQ, Li S, He JM (2020) UV RESISTANCE LOCUS8 mediates ultraviolet-B-induced stomatal closure in an ethylene-dependent manner. Plant Sci 301:110679

Hajdu A, Ádám É, Sheerin DJ, Dobos O, Bernula P, Hiltbrunner A, Kozma-Bognár L, Nagy F (2015) High-level expression and phosphorylation of phytochrome B modulates flowering time in Arabidopsis. Plant J 83:794–805

Heng YQ, Jiang Y, Zhao XH, Zhou H, Wang XC, Deng XW, Xu DQ (2019) BBX4, a phyB-interacting and modulated regulator, directly interacts with PIF3 to fine tune red light-mediated photomorphogenesis. Proc Natl Acad Sci USA 116:26049–26056

Hu LL, Liu P, Jin ZS, Sun J, Weng YQ, Chen P, Du SL, Wei AM, Li YH (2021) A mutation in *CsHY2* encoding a phytochromobilin (*PΦB*) synthase leads to an elongated hypocotyl 1 (*elh1*) phenotype in cucumber (*Cucumis sativus* L.). Theor Appl Genet 134:2639–2652

Huq E, Quail PH (2002) PIF4, a phytochrome-interacting bHLH factor, functions as a negative regulator of phytochrome B signaling in *Arabidopsis*. EMBO J 21:2441–2450

Inoue SI, Kaiserli E, Zhao X, Waksman T, Takemiya A, Okumura M, Takahashi H, Seki M, Shinozaki K, Endo Y, Sawasaki T, Kinoshita T, Zhang X, Christie JM, Shimazaki KI (2020) CIPK23 regulates blue light-dependent stomatal opening in *Arabidopsis thaliana*. Plant J 104:679–692

Iñigo S, Alvarez MJ, Strasser B, Califano A, Cerdán PD (2011) PFT1, the MED25 subunit of the plant mediator complex, promotes flowering through *CONSTANS* dependent and independent mechanisms in Arabidopsis. Plant J 69:601–612

Jang IC, Henriques R, Seo HS, Nagatani A, Chua NH (2010) *Arabidopsis* PHYTOCHROME INTERACTING FACTOR proteins promote phytochrome B polyubiquitination by COP1 E3 ligase in the nucleus. Plant Cell 22:2370–2383

Jung C, Müller AE (2009) Flowering time control and applications in plant breeding. Trends Plant Sci 14:563–573

Kahle N, Sheerin DJ, Fischbach P, Koch LA, Schwenk P, Lambert D, Rodriguez R, Kerner K, Hoecker U, Zurbriggen MD, Hiltbrunner A (2020) COLD REGULATED 27 and 28 are targets of CONSTITUTIVELY PHOTOMORPHOGENIC 1 and negatively affect phytochrome B signalling. Plant J 104:1038–1053

Kippes N, Vangessel C, Hamilton J, Akpinar A, Budak H, Dubcovsky J, Pearce S (2020) Effects of *phyB* and *phyC* loss-of-function mutations on the wheat transcriptome under short and long day photoperiods. BMC Plant Biol 20:297

Koornneef M, Rolff E, Spruit CJP (1980) Genetic control of light-inhibited hypocotyl elongation in *Arabidopsis thaliana* (L.) Heynh. Z Pflanzenphysiol 100:147–160

Kumar A, Singh A, Panigrahy M, Sahoo PK, Panigrahi-Kishore CS (2018) Carbon nanoparticles influence photomorphogenesis and flowering time *in Arabidopsis thaliana*. Plant Cell Rep 37:901–912

Lazaro A, Mouriz A, Piñeiro M, Jarillo JA (2015) Red light-mediated degradation of CONSTANS by the E3 ubiquitin ligase HOS1 regulates photoperiodic flowering in Arabidopsis. Plant Cell 27:2437–2454

Lee IJ, Foster KR, Morgan PW (1998a) Photoperiod control of gibberellin levels and flowering in sorghum. Plant Physiol 116:1003–1011

Lee IJ, Foster KR, Morgan PW (1998b) Effect of gibberellin biosynthesis inhibitors on native gibberellin content, growth and floral initiation in *Sorghum bicolor*. J Plant Growth Regul 17:185–195

Lee YS, Jeong DH, Lee DY, Yi J, Ryu CH, Kim SL, Jeong HJ, Choi SC, Jin P, Yang J, Cho LH, Choi H, An G (2010) *OsCOL4* is a constitutive flowering repressor upstream of *Ehd1* and downstream of *OsphyB*. Plant J 63:18–30

Leivar P, Quail PH (2011) PIFs: pivotal components in a cellular signaling hub. Trends Plant Sci 16:19–28

Li XY (2011) Infiltration of *Nicotiana benthamiana* protocol for transient expression via *Agrobacterium*. Bio-Protoc 1:1–3

Li YH, Wen CL, Weng YQ (2013) Fine mapping of the pleiotropic locus B for black spine and orange mature fruit color in cucumber identifies a 50 kb region containing a R2R3-MYB transcription factor. Theor Appl Genet 126:2187–2196

Liu B, Weng JY, Guan DL, Zhang Y, Niu QL, López-Juez E, Lai YS, Garcia-Mas J, Huang DF (2021a) A domestication-associated gene, *CsLH*, encodes a phytochrome B protein that regulates hypocotyl elongation in cucumber. Mol Hortic 1:3

Liu SR, Yang LW, Li JL, Tang WJ, Li JG, Lin RC (2021b) FHY3 interacts with phytochrome B and regulates seed dormancy and germination. Plant Physiol 187:289–302

Livak KJ, Schmittgen TD (2001) Analysis of relative gene expression data using real-time quantitative PCR and the $2^{-\Delta\Delta Ct}$ method. Methods 25:402–408

Lu HF, Lin T, Klein J, Wang SH, Qi JJ, Zhou Q, Sun JJ, Zhang ZH, Weng YQ, Huang SW (2014) QTL-seq identifies an early flowering QTL located near *Flowering Locus T* in cucumber. Theor Appl Genet 127:1491–1499

Lu X, Zhou C, Xu P, Luo Q, Lian H, Yang H (2015) Red light-dependent interaction of phyB with SPA1 promotes COP1-SPA1 dissociation and phoeomorphogenic development in *Arabidopsis*. Mol Plant 8:467–478

Mao ZL, He SB, Xu F, Wei XX, Jiang L, Wang WX, Li T, Xu PB, Du SS, Li L, Lian HL, Guo TT, Yang HQ (2020) Photoexcited CRY1 and phyB interact directly with ARF6 and ARF8 to regulate their DNA-binding activity and auxin-induced hypocotyl elongation in Arabidopsis. New Phytol 225:848–865

Miao TT, Li DZ, Huang ZY, Huang YW, Li SS, Wang Y (2021) Gibberellin regulates UV-B-induced hypocotyl growth inhibition in *Arabidopsis thaliana*. Plant Signal Behav 16:1966587

Miao LX, Zhao JC, Yang GQ, Xu P, Cao XL, Du SS, Xu F, Jiang L, Zhang SL, Wei XX, Liu Y, Chen HR, Mao ZL, Guo TT, Kou S, Wang WX, Yang HQ (2022) *Arabidopsis* cryptochrome 1 undergoes COP1 and LRBs-dependent degradation in response to high blue light. New Phytol 234:1347–1362

Ming CH, Jiang FL, Hu HM, Zhou XC, Zhan FH, Wu Z (2011) Effects of different leggy extent seedling on cucumber growth, yield and quality. China Veg 4:29–34 (**In Chinese**)

Mockler TC, Guo H, Yang H, Duong H, Lin C (1999) Antagonistic actions of *Arabidopsis cryptochromes* and phytochrome B in the regulation of floral induction. Development 126:2073–2082

Nagatani A (2010) Phytochrome: structural basis for its functions. Curr Opin Plant Biol 13:565–570

Nakano T (2019) Hypocotyl elongation: a molecular mechanism for the first event in plant growth that influences its physiology. Plant Cell Physiol 60:933–934

Nemhauser J, Chory J (2002) Photomorphogenesis the Arabidopsis. Book 1:e0054

Oda A, Fujiwara S, Kamada H, Coupland G, Mizoguchi T (2004) Antisense suppression of the *Arabidopsis PIF3* gene does not affect circadian rhythms but causes early flowering and increases *FT* expression. FEBS Lett 557:259–264

Oh J, Park E, Song K, Bae G, Choi G (2020) Phytochrome interacting factor 8 inhibits phytochrome A-mediated far-red light responses in Arabidopsis. Plant Cell 32:186–205

Pan Y, Qu SP, Bo KL, Gao ML, Haider KR, Weng Y (2017) QTL mapping of domestication and diversifying selection related traits in round-fruited semi-wild Xishuangbanna cucumber (*Cucumis sativus* L. var. xishuangbannanesis). Theor Appl Genet 130:1531–1548

Pearce S, Kippes N, Chen A, Debernardi JM, Dubcovsky J (2016) RNA-seq studies using wheat *PHYTOCHROME B* and *PHYTOCHROME C* mutants reveal shared and specific functions in the regulation of flowering and shade-avoidance pathways. BMC Plant Biol 16:141

Quail PH (2002) Phytochrome photosensory signalling networks. Nat Rev Mol Cell Biol 3:85–93

Reed JW, Nagpal P, Poole DS, Furuya M, Chory J (1993) Mutations in the gene for red/far-red light receptor phytochrome B alter cell elongation and physiological responses throughout *Arabidopsis* development. Plant Cell 5:147–157

Ren Y, Zhang Z, Liu J, Staub JE, Han Y, Cheng Z, Li X, Lu J, Miao H, Kang H, Xie B, Gu X, Wang X, Du C, Jin W, Huang S (2009) An integrated genetic and cytogenetic map of the cucumber genome. PLoS ONE 4:e5795

Robbins MD, Staub JE (2009) Comparative analysis of marker-assisted and phenotypic selection for yield components in cucumber. Theor Appl Genet 119:621–634

Rusaczonek A, Czarnocka W, Willems P, Sujkowska-Rybkowska M, Breusegem FN, Karpiński S (2021) Phototropin 1 and 2 influence photosynthesis, UV-C induced photooxidative stress responses, and cell death. Cells 10:200

Saitou N, Nei M (1987) The neighbor-joining method: a new method for reconstructing phylogenetic trees. Mol Biol Evol 4:406–425

Sheerin DJ, Menon C, Oven-Krockhaus SZ, Enderle B, Zhu L, Johnen P, Schleifenbaum F, Stierhof YD, Huq E, Hiltbrunner A (2015) Light-activated phytochrome A and B interact with memebers of the SPA family to promote photomorphogenesis in Arabidopsis by reorganizing the COP1/SPA complex. Plant Cell 27:189–201

Shen H, Zhu L, Castillon A, Majee M, Downie B, Huq E (2008) Light-induced phosphorylation and degradation of the negative regulator PHYTOCHROME-INTERACTING FACTOR1 from Arabidopsis depend upon its direct physical interactions with photoactivated phytochromes. Plant Cell 20:1586–1602

Sheng YY, Pan YP, Li YH, Yang LM, Weng YQ (2019) Quantitative trait loci for fruit size and flowering time-related traits under domestication and diversifying selection in cucumber (*Cucumis sativus*). Plant Breeding 139:176–191

Song YH, Shim JS, Kinmonth-Schultz HA, Imaizumi T (2015) Photoperiodic flowering: time measurement mechanisms in leaves. Annu Rev Plant Biol 66:441–464

Su L, Hou P, Song MF, Zheng X, Guo L, Xiao Y, Yan L, Li WC, Yang JP (2015) Synergistic and antagonistic action of phytochrome (Phy) A and PhyB during seedling de-etiolation in *Arabidopsis thaliana*. Int J Mol Sci 16:12199–12212

Sun WJ, Han HY, Deng L, Sun CL, Xu TR, Li LH, Ren PR, Zhao JH, Zhai QZ, Li CY (2020) Mediator subunit MED25 physically interacts with PHYTOCHROME INTERACTING FACTOR4 to regulate shade-induced hypocotyl elongation in tomato. Plant Physiol 184:1549–1562

Suzuki A, Suriyagoda L, Shigeyama T, Tominaga A, Sasaki M, Hiratsuka Y, Yoshinaga A, Arima S, Agarie S, Sakai T, Inada S, Jikumaru Y, Kamiya Y, Uchiumi T, Abe M, Hashiguchi M, Akashi R, Sato S, Kaneko T, Tabata S, Hirsh AM (2011) *Lotus japonicus* nodulation is photomorphogenetically controlled by sensing the red/far red (R/FR) ration through jasmonic acid (JA) signaling. Proc Natl Acad Sci USA 108:16837–16842

Takano M, Inagaki N, Xie XZ, Yuzurihara N, Hihara F, Ishizuka T, Yano M, Nishimura M, Miyao A, Hirochika H, Shinomura T (2005) Distinct and cooperative functions of phytochromes A, B, and C in the control of de-etiolation and flowering in rice. Plant Cell 17:3311–3325

Tuinen AV, Kerckhoffs LHJ, Nagatani A, Kendrick RE, Koornneef M (1995) A temporarily red light-insensitive mutant of tomato lacks a light-stable, B-like phytochrome. Plant Physiol 108:939–947

Wagner D, Koloszvari M, Quail PH (1996) Two small spatially distinct regions of phytochrome B are required for efficient signaling rates. Plant Cell 8:859–871

Wan H, Zhao Z, Qian C, Sui Y, Malik AA, Chen J (2010) Selection of appropriate reference genes for gene expression studies by quantitative real-time polymerase chain reaction in cucumber. Anal Biochem 399:257–261

Wang YH, Bo KL, Gu XF, Pan JS, Li YH, Chen JF, Wen CL, Ren ZH, Ren HZ, Chen XH, Grumet G, Weng Y (2019) Molecularly tagged

genes and quantitative trait loci in cucumber with recommendations for QTL nomenclature. Hortic Res 7:3

Wei XX, Wang WT, Xu P, Wang WX, Guo TT, Kou S, Liu MQ, Niu YK, Yang HQ, Mao ZL (2021) Phytochrome B interacts with SWC6 and ARP6 to regulate H2A.Z deposition and photomorphogenesis in *Arabidopsis*. J Integr Plant Biol 63:1133–1146

Wicker T, Sabot F, Hua-Van A, Bennetzen JL, Capy P, Chalhoub B, Flavell A, Leroy P, Morgante M, Panaud O, Paux E, Sanmiguel P, Schulman AH (2007) A unified classification system for eukaryotic transposable elements. Nat Rev Genet 8:973–982

Wollenberg AC, Strasser B, Cerdán PD, Amasino RM (2008) Acceleration of flowering during shade avoidance in Arabidopsis alters the balance between *FLOWERING LOCUS C*-mediated repression and photoperiodic induction of flowering. Plant Physiol 148:1681–1694

Valverde F, Mouradov A, Soppe W, Ravenscroft D, Samach A, Coupland G (2004) Photoreceptor regulation of CONSTANS protein in photoperiodic flowering. Science 303:1003–1006

Xu PB, Lian HL, Xu F, Zhang T, Wang S, Wang WX, Du SS, Huang JR, Yang HQ (2019) Phytochrome B and AGB1 coordinately regulate photomorphogenesis by antagonistically modulating PIF3 stability in *Arabidopsis*. Mol Plant 12:229–247

Xu P, Chen HR, Li T, Xu F, Mao ZL, Cao XL, Miao LX, Du SS, Hua J, Zhao JC, Guo TT, Kou S, Wang WX, Yang HQ (2021) Blue light-dependent interactions of CRY1 with GID1 and DELLA proteins regulate gibberellin signaling and photomorphogenesis in Arabidopsis. Plant Cell 33:2375–2394

Yadav A, Singh D, Lingwan M, Yadukrishnan P, Masakapalli SK, Datta S (2020) Light signaling and UV-B-mediated plant growth regulation. J Integr Plant Biol 62:1270–1292

Yan Y, Li C, Dong XJ, Li H, Zhang D, Zhou YY, Jiang BC, Peng J, Qin XY, Cheng JK, Wang XJ, Song PY, Qi LJ, Zheng Y, Li BS, Terzaghi W, Yang SH, Guo Y, Li JG (2020) MYB30 is a key negative regulator of Arabidopsis photomorphogenic development that promotes PIF4 and PIF5 protein accumulation in the light. Plant Cell 32:2196–2215

Yasui Y, Mukougawa K, Uemoto M, Yokofuji A, Suzuri R, Nishitani A, Kohchi T (2012) The phytochrome-interacting VASCULAR PLANT ONE-ZINC FINGER1 AND VOZ2 redundantly regulate flowering in Arabidopsis. Plant Cell 24:3248–3263

Yoshida Y, Sarmiento-Mañús R, Yamori W, Ponce MR, Micol JL, Tsukaya H (2018) The Arabidopsis *phyB-9* mutant has a second-site mutation in the *VENOSA4* gene that alters chloroplast size, photosynthetic traits, and leaf growth. Plant Physiol 178:3–6

Zhong M, Zeng BJ, Tang DY, Yang JX, Qu LN, Yan JD, Wang XC, Li X, Liu XM, Zhao XY (2021) The blue light receptor CRY1 interacts with GID1 and DELLA proteins to repress GA signaling during photomorphogenesis in Arabidopsis. Mol Plant 14:1328–1342

Zou Y, Li R, Baldwin IT (2020) ZEITLUPE is required for shade avoidance in the wild tobacco *Nicotiana attenuata*. J Integr Plant Biol 62:1341–1351